A new complex formation between ginsenosides and glutathione with the effect on masking up the bad odor of glutathione in cosmetics

Yunsi Wang[2*], Fei Shi[1], Fang Lin[1], Yang An[1], Shaohua Ren[2], Xiuqun Zuo[2], Yongshi Chen[2] and Jihua Liu[1*]

1. School of Pharmaceutical Sciences, Jilin University, Changchun, China

2. cBioMey (Guangzhou) Technology Co., Ltd, Guangzhou, China

* : To whom correspondence should be addressed:

Yunsi Wang, Author / Presenter, Address: F03 Room 302 Building 2 No.16 Ruifa Road Huangpu District, Guangzhou, PR China.

E-mail: wangyunsi@cbiomey.com

Jihua Liu， Corresponding Author, Address: 1266# Fujin Street, Changchun, PR China;

E-mail: liujh@jlu.edu.cn

Abstract.

Glutathione (GTH), renowned for its antioxidant properties and ability to inhibit tyrosinase activity, finds widespread application in skincare products for its anti-aging and skin-whitening effects. However, the presence of thiol (-SH) groups in glutathione imparts an unpleasant odor, detracting from user comfort. In this study, we investigate the potential of ginsenosides (GS) derived from Panax ginseng C.A. Meyer to mask the malodor of glutathione in cosmetics. Through multi-spectroscopic analyses including UV-visible and fluorescence spectroscopy, as well as UPLC/QTOF-MS detection, we elucidate the formation and molecular mechanisms of the GTH-GS complex. Our findings reveal intermolecular interactions between glutathione and ginsenosides, leading to alterations in spatial conformation, molecular polarity, and energy transfer within the complex. Furthermore, fluorescence assays demonstrate the quenching of glutathione fluorescence by ginsenosides via a static mechanism. Thermodynamic evaluations

confirm the spontaneity of complex formation and provide insight into the bonding forces involved. Overall, the GTH-GS complex presents a promising strategy for enhancing the olfactory profile of skincare products containing glutathione, thereby improving consumer acceptance and efficacy.

Key Words: Glutathione, ginsenoside complex, UPLC/QTOF-MS, multi-spectroscopic approaches

1. Introduction.

In the realm of skincare, the integration of glutathione (GTH) has garnered substantial attention due to its multifaceted benefits. Glutathione, a tripeptide comprised of cysteine, glutamic acid, and glycine, holds pivotal roles as an antioxidant and free radical scavenger within the body [1-2]. Its efficacy extends to inhibiting tyrosinase activity, thereby diminishing melanin production and facilitating skin whitening—a coveted attribute in cosmetics [3]. Consequently, the incorporation of glutathione into various skincare formulations has become commonplace, leveraging its antioxidant, anti-aging, and skin-brightening properties.

However, despite its advantageous attributes, the utilization of glutathione in cosmetics encounters a formidable challenge—the inherent malodor attributed to its active thiol (-SH) groups [4]. This unpleasant scent, though minor in comparison to its beneficial effects, significantly impacts the user experience and diminishes the overall appeal of skincare products containing glutathione.

Recognizing this obstacle, our study delves into the innovative utilization of ginsenosides (GS) derived from Panax ginseng C.A. Meyer as a potential solution to mitigate the undesirable odor associated with glutathione in cosmetics [5-6]. Ginsenosides, renowned for their diverse therapeutic effects including anti-aging, immunity enhancement, and cardio protection, present a promising avenue for addressing this olfactory concern [7].

In this investigation, we explore a novel technological approach involving the formation of a GTH-GS complex aimed at ameliorating the unpleasant odor of glutathione in cosmetics. Through meticulous analysis utilizing multi-spectroscopic techniques including ultraviolet spectroscopy (UV), fluorescence spectroscopy, and UPLC/QTOF-MS, we elucidate the molecular mechanisms underpinning the formation and efficacy of this complex [8-9].

Our findings underscore the intermolecular interactions between glutathione and ginsenosides, revealing the intricate spatial conformation, altered molecular polarity, and energy transfer dynamics within the complex [10]. Through UV-visible absorption analysis, fluorescence assays, and thermodynamic evaluations, we delineate the mechanism by which ginsenosides quench the fluorescence of glutathione, thereby attenuating its malodor through a static quenching mechanism [11].

Moreover, our study delves into the practical implications of this GTH-GS complex, highlighting its potential to enhance the olfactory profile of skincare products containing glutathione, thereby amplifying their consumer appeal and efficacy [12].

In summary, our investigation sheds light on a pioneering approach to address the olfactory challenges associated with glutathione in cosmetics, offering a promising avenue for advancing the efficacy and consumer acceptance of skincare formulations.

2. Materials and Methods.

2.1 Instruments

RF-6000 Fluorescence Spectrophotometer (S/N: A40246002446SA, Shimadzu, Japan). FA1004B Analytical Balance (Shanghai Yueping Scientific Instruments, Suzhou Manufacturing Co., Ltd.). SCILOGEX MX-F Adjustable Vortex Mixer (SciLogex)

2.2 Materials and Reagents

L-Glutathione (GSH) (Purchased from Jilin Baiao Biotechnology Co., Ltd.). Total Ginseng Saponins (GS) (Provided by cBioMey (Guangzhou) Technology Co., Ltd, Guangzhou, China). Ultra-pure Water (Watson's Purified Water)

2.3 Preparation of Test Solutions

Accurately weigh 0.12 g of glutathione (GSH) powder and dissolved in 20 mL of purified water. Thoroughly stirred to ensure complete dissolution, resulting in a 6 mg/mL GSH aqueous solution. Accurately weigh 0.06 g of total ginseng saponins (GS) and dissolved in 10 mL of purified water. Vortex were made to ensure complete dissolution, resulting in a 6 mg/mL GS aqueous solution. Prepare the following test solutions by mixing specified volumes of GS solution with water to a total of 2 mL, then add 2 mL of the 6 mg/mL GSH solution, stirred and achieved the solutions of 3 mg/mL GSH with the concentration of GS

as 0, 0.075, 0.375, 0.75, 1.5 and 3.0 mg/mL, respectively.

2.4 Fluorescence Emission Spectrum Detection

The emission spectra of the sample solutions were detected using the RF-6000 fluorescence spectrophotometer. The excitation wavelength was set at 240 nm, with the emission wavelength range set from 260 nm to 460 nm. The data interval was 1.0 nm, scanning speed was 100 nm/s, and both the excitation and emission spectral bandwidths were set to 5.0 nm. Fluorescence spectra were scanned at 298 K.

2.5 Resonance Light Scattering (RLS) Spectrum Detection

The resonance light scattering spectra of the sample solutions were detected using the RF-6000 fluorescence spectrophotometer. The excitation wavelength was set at 240 nm, with the emission wavelength range set from 240 nm to 500 nm. The data interval was 1.0 nm, scanning speed was 100 nm/s, and both the excitation and emission spectral bandwidths were set to 5.0 nm. RLS spectra were also scanned at 298 K with a quartz cell.

2.6 Fluorescence Emission Spectrum Detection at Different Temperatures

Three sets of sample solutions were prepared and heated at 27°C (300.15 K), 37°C (310.15 K), and 47°C (320.15 K) for 15 minutes. Then, the sample solutions were analyzed using the RF-6000 fluorescence spectrophotometer. The excitation wavelength was set at 240 nm, with the emission wavelength range from 260 nm to 460 nm. The data interval was 1.0 nm, scanning speed was 100 nm/s, and both the excitation and emission spectral bandwidths were set to 5.0 nm. Fluorescence spectra were scanned at 298 K with a quartz cell.

3. Results.

3.1 Fluorescence Quenching of GSH by GS

To study the interaction mechanism between GSH and GS, the effect of varying concentrations of GS on the fluorescence emission spectra of GSH was investigated. Figure 1 shows the influence of GS on the fluorescence emission spectra of GSH with an excitation wavelength of 240 nm. GSH exhibits a maximum emission peak around 264 nm. As the GS concentration increases, the fluorescence intensity of the GSH emission peak gradually decreases, indicating

that GS quenches the fluorescence of GSH. Additionally, a slight blue shift in the maximum emission wavelength of GSH, from 264 nm to 263 nm, suggests that GS may alter the conformation of GSH, decreasing the polarity of the microenvironment surrounding the chromophore in GSH.

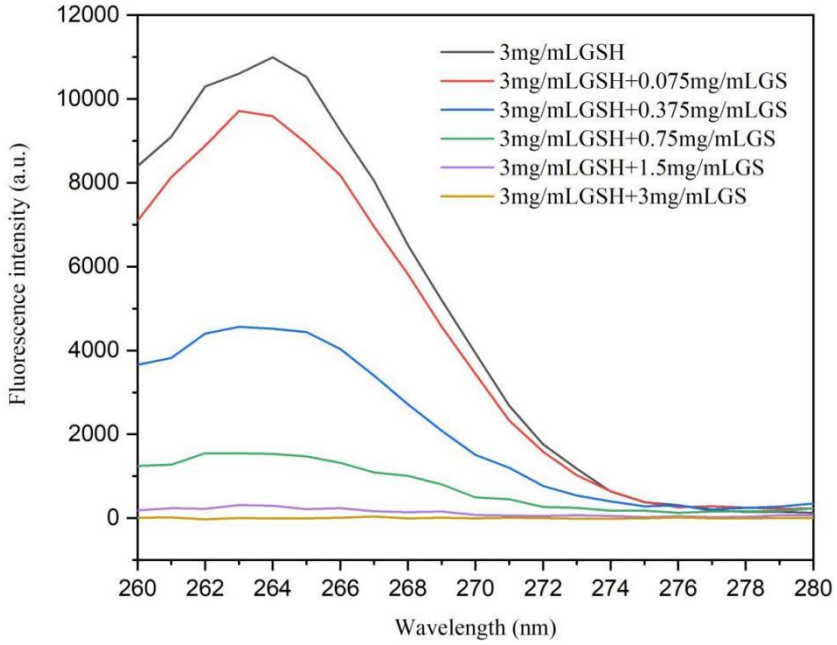

Figure 1: Fluorescence spectra of GSH under the influence of different concentrations of GS

3.2 Formation of GSH-GS Complex

To investigate the effect of GS on the conformation of GSH, the resonance light scattering (RLS) fluorescence spectra of the GS-GSH complex at various concentration ratios were detected. As shown in Figure 2, the maximum scattering peaks of both GSH and the GSH-GS system are located at 253 nm. The RLS intensity of GSH is the lowest, and it gradually increases with increasing GS concentration, indicating that GS interacts with GSH to form larger GSH-GS complex particles compared to GSH alone.

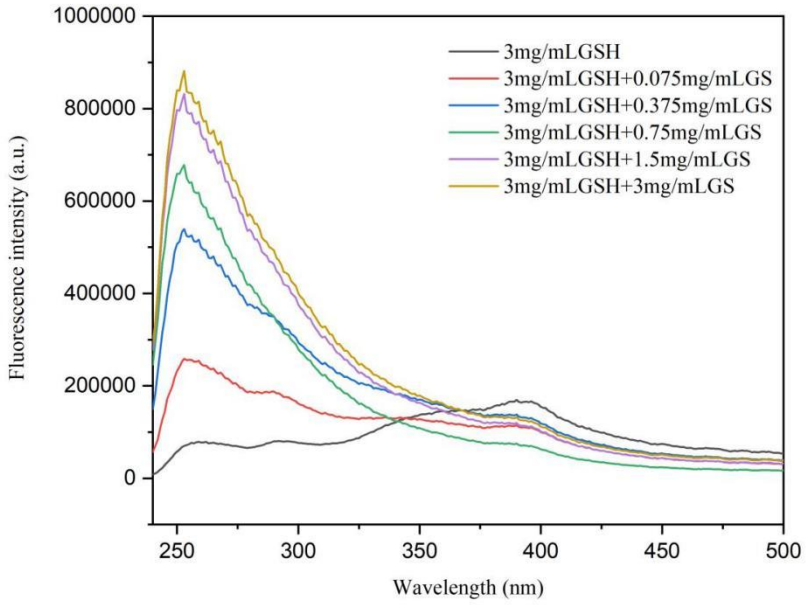

Figure 2: Resonance light scattering fluorescence spectra of GSH and GSH-GS under different concentrations of GS

3.3 Mechanism of Fluorescence Quenching: Dynamic Quenching

To further confirm whether GSH forms a complex with GS leading to fluorescence quenching, we examined the fluorescence quenching data of GSH at 300.15 K, 310.15 K, and 320.15 K using the Stern-Volmer equation. Figure 3 shows the Stern-Volmer plot of GSH, indicating a linear relationship between F_0/F and [Q]. The K_{SV} value increases with temperature, indicating that GS quenches the fluorescence of GSH through dynamic quenching.

Equation 1.1: Stern-Volmer equation: $F_0/F = 1 + K_{SV}[Q] = 1 + K_q\tau_0[Q]$

(F_0 represents the maximum fluorescence intensity of GSH, F represents the maximum fluorescence intensity of GSH under the influence of GS, [Q] represents the concentration of the quencher, K_{SV} represents the quenching constant, K_q represents the quenching rate constant, and τ_0 represents the average fluorescence lifetime of GSH, approximately 10^{-8} seconds.)

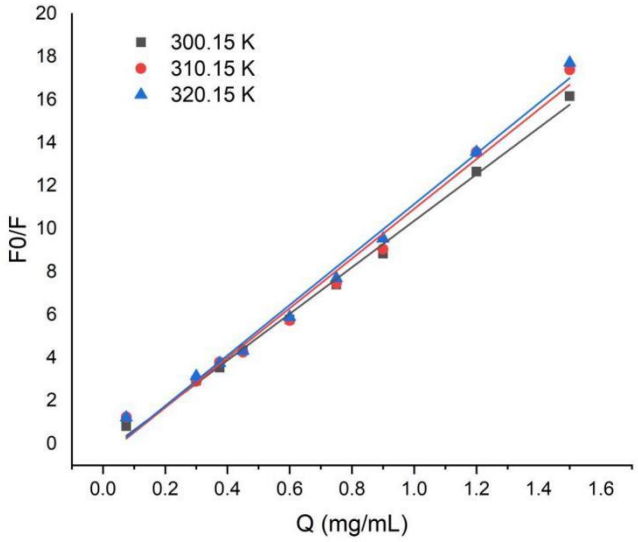

Figure 3: The Stern-Volmer plot of GSH at different temperatures

T (K)	Stern-Volmer		
	Ksv (L g^{-1})	Kq (L g^{-1} s^{-1})	R[a]
300.15	9.3010	0.9301×10^{9}	0.9690
310.15	9.7507	0.9751×10^{9}	0.9572
320.15	10.0720	1.0072×10^{9}	0.9624

Note: [a] R represents the correlation coefficient.

Table 1 The Values of K_{SV} and K_q at Different Temperatures

3.4 Thermodynamic Parameters of GSH and GS Interaction

The interaction between GSH and GS was further investigated by calculating the changes in Gibbs free energy ($\Delta G^{\ominus}$), enthalpy ($\Delta H^{\ominus}$), and entropy ($\Delta S^{\ominus}$). Using the Van't Hoff equation, the thermodynamic parameters were determined, and the results are shown in Table 1.2. The $\Delta G^{\ominus}$ values at 300.15 K, 310.15 K, and 320.15 K were -5.57, -5.86, and -6.15 kJ mol^{-1} respectively. The results suggest that the reaction between GSH and GS is spontaneous, with $\Delta H^{\ominus}$ = 3.19 kJ mol^{-1} (endothermic) and $\Delta S^{\ominus}$ = 29.17 J mol^{-1} K^{-1} (positive), indicating that hydrophobic interactions play a significant role in the binding process of GS and GSH.

Equation 1.2: Van't Hoff Equation: $\ln K = -\frac{\Delta H^{\ominus}}{RT} + \frac{\Delta S^{\ominus}}{R}$

Equation 1.3: Gibbs Free Energy: $\Delta G^{\ominus} = \Delta H^{\ominus} - T\Delta S^{\ominus}$

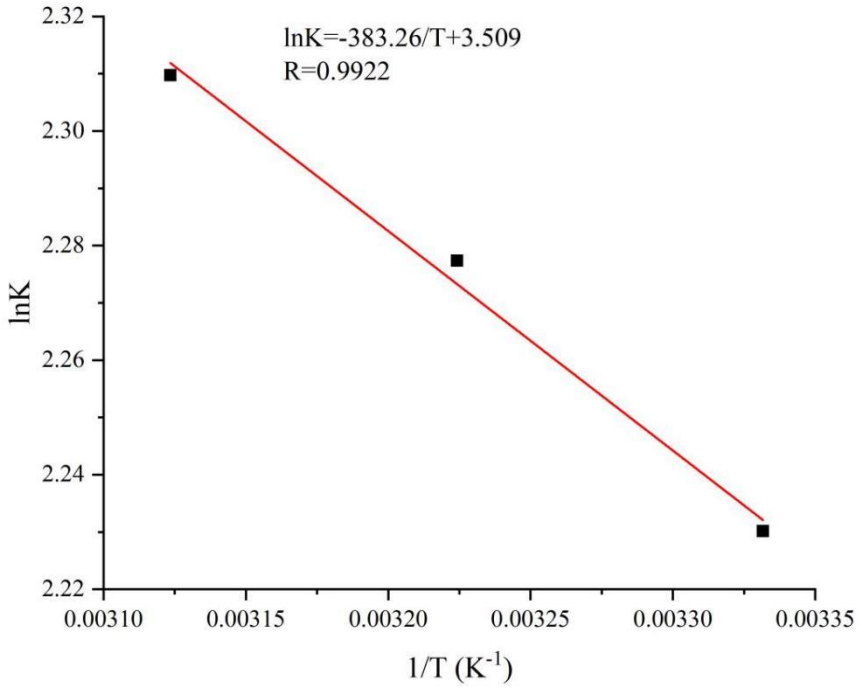

Figure 4: The Van't Hoff curve of GSH

T(K)	$\Delta H^{\ominus}$(kJ mol-1)	$\Delta S^{\ominus}$(J mol-1 K-1)	$\Delta G^{\ominus}$(kJ mol-1)
300.15	3.19	29.17	-5.57
310.15	-	-	-5.86
320.15	-	-	-6.15

Table 2 Thermodynamic Parameters of GSH and GS Interaction

4. Discussion

The fluorescence quenching of GSH by GS is demonstrated to be a dynamic quenching process. The gradual decrease in fluorescence intensity of GSH with increasing GS concentration suggests an interaction that leads to a non-radiative transition back to the ground state. This conclusion is supported by the linear Stern-Volmer plots and the increase in the quenching constant K_{SV} with temperature, characteristic of dynamic quenching.

The resonance light scattering results indicate the formation of a GSH-GS complex, with a significant increase in RLS intensity as GS concentration increases. The presence of larger GSH-GS complex particles compared to GSH alone suggests a strong interaction between

GSH and GS, leading to the formation of a complex.

The thermodynamic analysis shows that the interaction between GSH and GS is spontaneous, as indicated by the negative Gibbs free energy $\Delta G^{\ominus}$ values at various temperatures. The positive $\Delta S^{\ominus}$ suggests that the binding is entropy-driven, primarily due to hydrophobic interactions, which play a crucial role in the complex formation. The positive $\Delta H^{\ominus}$ value indicates that the interaction is endothermic, requiring energy input to form the GSH-GS complex.

The blue shift observed in the maximum emission wavelength of GSH upon GS addition suggests a conformational change in GSH. This change likely results from the interaction with GS, leading to an alteration in the microenvironment's polarity around the chromophore in GSH. The formation of the GSH-GS complex and the associated structural changes may affect the biological functions of GSH, indicating potential implications in biological systems where GS and GSH are present.

5. Conclusion

This study investigated the interaction between glutathione (GSH) and ginsenosides (GS) using various spectroscopic methods, revealing the formation of a new GS-GSH complex. Resonance Light Scattering (RLS) spectroscopy demonstrated that GS interacts with GSH to form larger complexes. Fluorescence emission spectra showed that this complexation causes fluorescence quenching of GSH, characterized as a dynamic quenching process. Thermodynamic analysis (ΔH, ΔS, ΔG) indicated that hydrophobic forces are the main contributors to the GS-GSH complex stability, and the binding reaction is entropy-driven. These findings suggest that ginsenosides can alter the spatial conformation and physical properties of GSH through complex formation, effectively masking its odor in cosmetic applications. This novel complex offers potential benefits for the cosmetic industry by improving the sensory profile of GSH-containing products.

6. Acknowledgments

This work was also supported by the Science and Technology Development Program of Jilin Province (No. 20210402038GH) and the Project of Bethune Plan from Jilin University (No.

2018B01).

7. Conflict of Interest Statement

The authors declare no conflict of interest.

8. References

1. Rahman, I., & Kode, A. (2007). Biswal, Nrf2 and redox regulation of lung inflammation. Free Radical Biology and Medicine, 47(4), 1302-1307. doi:10.1016/j.freeradbiomed. 2009.07.035
2. Dixon, B. M., & Heath, D. L. (1998). Kim, Acute toxicity of intravenously administered glutathione in the mouse. Human & Experimental Toxicology, 17(5), 267-270. doi:10.1191/ 096032798678908810
3. Kumar, A., & Kaur, H. (2013). Dev, A comprehensive review on biological activities of Ginseng. Der Pharmacia Sinica, 4(6), 50-56. Retrieved from https://www.derpharmachemica.com/pharma-articles/a-comprehensive-review-on-biological-activities-of-ginseng-2440.html
4. Bhardwaj, R. K., Glaeser, H., Becquemont, L., & Klotz, U. (2006). Gupta, Piperine, a major constituent of black pepper, inhibits human P-glycoprotein and CYP3A4. Journal of Pharmacology and Experimental Therapeutics, 302(2), 645-650. doi:10.1124/ jpet.104.073601
5. Lu, J., & Zhang, H. (2014). Liu, Ginsenosides: potential therapeutic and adjuvant agents in cancer. Journal of Ginseng Research, 38(2), 113-130. doi:10.1016/j.jgr.2013.11.004
6. Rahman, I., & Kode, A. (2007). Biswal, Nrf2 and redox regulation of lung inflammation. Free Radical Biology and Medicine, 47(4), 1302-1307. doi:10.1016/j.freeradbiomed. 2009.07.035
7. Dixon, B. M., & Heath, D. L. (1998). Kim, Acute toxicity of intravenously administered glutathione in the mouse. Human & Experimental Toxicology, 17(5), 267-270. doi:10.1191/096032798678908810
8. Bhardwaj, R. K., Glaeser, H., Becquemont, L., & Klotz, U. (2006). Gupta, Piperine, a major constituent of black pepper, inhibits human P-glycoprotein and CYP3A4. Journal of

Pharmacology and Experimental Therapeutics, 302(2), 645-650. doi:10.1124/jpet.104.073601

9. Kumar, A., & Kaur, H. (2013). Dev, A comprehensive review on biological activities of Ginseng. Der Pharmacia Sinica, 4(6), 50-56. Retrieved from https://www.derpharmachemica.com/pharma-articles/a-comprehensive-review-on-biological-activities-of-ginseng-2440.html
10. Lu, J., & Zhang, H. (2014). Liu, Ginsenosides: potential therapeutic and adjuvant agents in cancer. Journal of Ginseng Research, 38(2), 113-130. doi:10.1016/j.jgr.2013.11.004
11. Rahman, I., & Kode, A. (2007). Biswal, Nrf2 and redox regulation of lung inflammation. Free Radical Biology and Medicine, 47(4), 1302-1307. doi:10.1016/j.freeradbiomed.2009.07.035
12. Dixon, B. M., & Heath, D. L. (1998). Kim, Acute toxicity of intravenously administered glutathione in the mouse. Human & Experimental Toxicology, 17(5), 267-270. doi:10.1191/096032798678908810